



Case Study

Assessment of soil liquefaction potential: a case study for Moulvibazar town, Sylhet, Bangladesh

Md. Shakhawat Hossain¹ · A. S. M. Maksud Kamal¹ · Md. Zillur Rahman¹ · Atikul Haque Farazi² · Dhiman Ranjan Mondal³ · Tonoy Mahmud¹ · Nasim Ferdous¹

Received: 31 December 2019 / Accepted: 20 March 2020
© Springer Nature Switzerland AG 2020

Abstract

Liquefaction can intensify the destruction caused by an earthquake; thus, a region with high liquefaction potential could be more disastrous. Bangladesh is surrounded by the Indo-Burma Folded Belt in the east, the Dauki Fault and Himalayan Syntaxis in the north that are known to have occurred high magnitude earthquakes (e.g., $M_w > 7$) in the past. Therefore, assigning seismic hazards in the regions that are economically growing fast is of great interest. Among many other hazard assessment parameters, soil liquefaction potential index (LPI) can be used to assess seismic hazards. In this study, we have assessed the seismic hazard potential for a small town (Moulvibazar) in the northeast Bangladesh documenting liquefaction potential indices for different surface geological units using an earthquake of moment magnitude M_w 8 having a peak horizontal ground acceleration (PGA) of 0.36 g. Twenty-five standard penetration test (SPT) boreholes were completed within the study area to obtain SPT-N values for two surface geological units: (1) Holo–Pleistocene low elevated terrace deposits (Zone 1) and (2) Holocene flood plain deposits (Zone 2). Using the SPT-N values, the LPI values have been calculated for the soil profile of each borehole. The LPI values in the town vary from 0 to 42.33, whereas values from 1.42 to 7.52 are in Zone 1 and values from 0 to 42.34 are in Zone 2. It has been predicted that 42% and 78% areas of Zone 1 and Zone 2, respectively, might exhibit surface manifestation of liquefaction. The results of this study can be used for seismic risk management of Moulvibazar town.

Keywords Earthquake · Liquefaction · Surface geology · Standard penetration test (SPT) · Simplified procedure · Liquefaction potential index (LPI)

1 Introduction

Liquefaction can cause extensive damage during an earthquake. The 2018 Sulawesi Earthquake in Indonesia, 1999 Chi-Chi Earthquake in Taiwan, 1989 Loma Prieta and 1964 Alaska Earthquakes in USA, 1964 Niigata Earthquake in Japan have revealed how soil liquefaction can increase the intensity of the damage caused by seismic shaking [10, 19, 21, 34, 36, 38, 46]. Therefore, it is necessary to assess the liquefaction potential of earthquake prone areas where

water-saturated Quaternary loose sediments exist down to a depth of 20 m.

About 80% landmass of Bangladesh is covered by the Quaternary loose and soft sediments [3]. Extensive liquefaction phenomena were documented in alluvial deposits of Bangladesh after the 1885 Bengal Earthquake, 1897 Great Indian Earthquake, and 1918 Srimangal Earthquake [23, 29, 42]. Paleoseismic investigations revealed liquefaction phenomena in the northern and northeastern parts of the country, which are believed

✉ Md. Zillur Rahman, zillur@du.ac.bd | ¹Department of Disaster Science and Management, University of Dhaka, Dhaka 1000, Bangladesh. ²Department of Geology and Mining, University of Barisal, Barishal 8200, Bangladesh. ³MIT Haystack Observatory, Westford, MA 01886, USA.



to be caused by a number of seismic events along the Dauki fault [25–27]. Earthquake of moderate to large magnitude may occur in this region as a result of continuing tectonic deformation along the active Indo-Burman plate-boundary faults [24, 41]. The northeast region of Bangladesh is the most vulnerable to earthquake given that this region is close to the two potential sources, i.e., Dauki Fault [26] and Indo-Burma Fold Belt [41].

In the present study, liquefaction potential of Moulvibazar, a rapidly growing district town in the northeastern part of the country, has been evaluated for future urban planning and development of the town Fig. 1. The seismic zoning map of Bangladesh [8] delineated this town within the most vulnerable seismic hazard prone zone of Bangladesh, where the peak horizontal ground acceleration (PGA) value is assigned as 0.36 g. The subsurface soils of the town down to a depth of more than 20 m are composed of the Holo–Pleistocene and Holocene loose and soft sediments [32]. The epicenter of the 1918 Srimangal Earthquake (M_w 7.6) was close to Moulvibazar town, and extensive liquefaction phenomena were observed in this region including the town area after this quake [42, 43]. Therefore, liquefaction potential assessment for the town is essential for a safe and resilient urban development. Present study is aimed at preparing an earthquake-induced soil liquefaction hazard map for Moulvibazar town using a design

earthquake of M_w 8 having a horizontal peak ground acceleration (PGA) of 0.36 g.

Earthquake-induced soil liquefaction potential is generally evaluated from standard penetration test blow counts (SPT-N) using the simplified procedure that was originally proposed by Seed and Idriss [37]. Later, the simplified procedure has been updated, calibrated, and validated by many researchers [48]. The procedure is applied to estimate the factor of safety (F_L) against liquefaction, where $F_L > 1$ designates that a soil layer will not liquefy and $F_L < 1$ indicates that a layer will liquefy during cyclic loading [30, 37]. Iwasaki et al. [16] introduced liquefaction potential index (LPI), where F_L is a function of the thickness of liquefiable layer and depth of the layer from the ground surface.

Although this region has high potentiality to cause earthquake-induced liquefaction, no study has been conducted yet to assess the liquefaction hazard for this town of Bangladesh. Therefore, the infrastructures of the town are being constructed without considering seismic and liquefaction hazard. Present study attempts to assess the factor of safety of liquefaction using simplified procedure [48] to figure out liquefaction potential index (LPI) for the subsurface geological materials of Moulvibazar town. The factors of safety of liquefaction for various soil layers are evaluated using a scenario earthquake of M_w 8.0 having a PGA value of 0.36 g to estimate the LPI value of the soil profiles. A liquefaction hazard map has been prepared

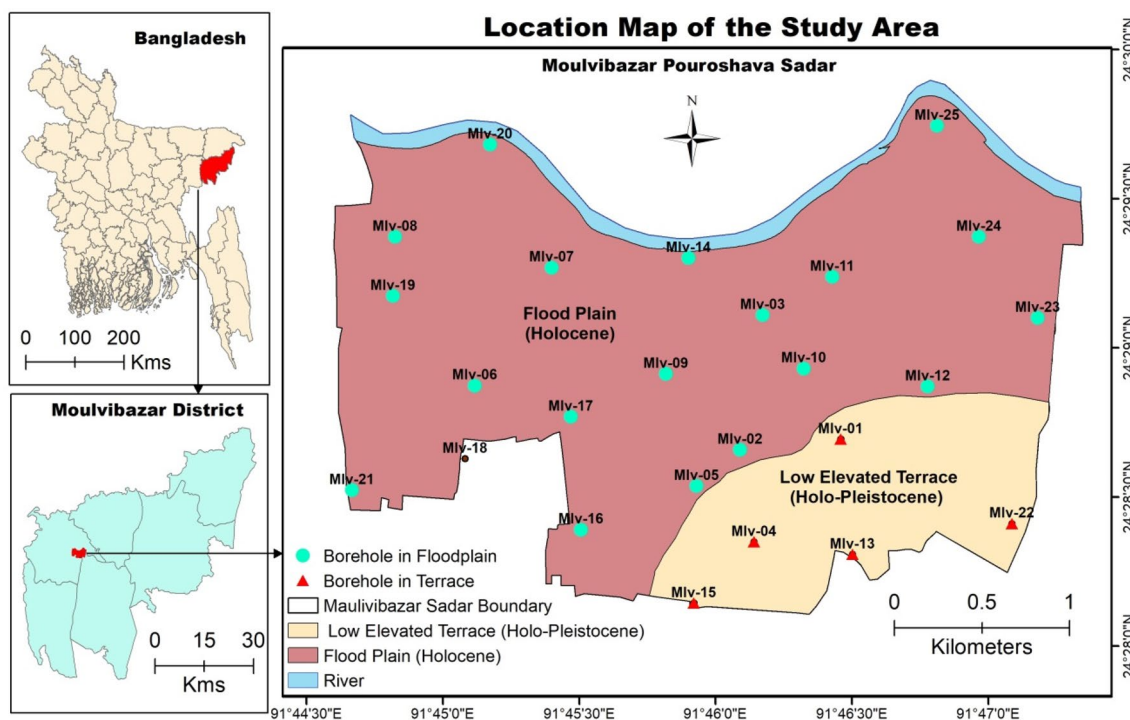


Fig. 1 Location map and surface geology map along with the borehole locations in Moulvibazar town

using contour lines of the LPI values, and the cumulative frequency distribution (CFD) of the LPI values of different surface geological units.

2 Study area

Moulvibazar town is located on the bank of the Manu River in the northeastern part of Bangladesh Fig. 1. The town has its present area of about 10.36 km² and total population of about 56,537 with population density of 5,457 per square kilometer [5]. It is further growing rapidly with increase in both population and masonry structures.

2.1 Geomorphology and geology

From the geomorphological point of view, this town is characterized by a landscape with Holocene flood plain, low elevated terrace, and sporadic hillocks [32]. As seismic hazard assessment and site characterization are still at nascent state in Bangladesh, it is no wonder that this rapidly growing town is still lacking investigation as per the risk assessment of ground failure by seismic soil liquefaction hazard.

The area exhibits two major surface geological units: the Holo–Pleistocene low elevated terrace and Holocene flood plain deposits Fig. 1. The Holo–Pleistocene low elevated terrace unit occupies the southeastern corner of the town, while the Holocene flood plain unit covers the rest of the area of the town. Table 1 represents soil classification of the geological materials of Moulvibazar town according to the Unified Soil Classification System (USCS), and their geologic ages. Among them, the Holocene terrace deposits are mainly composed of silty clay, clayey silt, and sand. The sand grains are generally medium to fine grained. Mineralogical composition of the geological materials of this unit is chiefly quartz, feldspar, mica, and dark colored minerals. This unit covers about 7.00 km² area of the town and has elevation of 13–20 m. On the other hand, the Holo–Pleistocene low elevated terrace deposits are chiefly comprised of clayey silt to silty clay with sand. Mottling of color is present in these red to yellowish red and grey geological materials. This unit covers 3.00 km² area of the town with elevation varying from 13 to 25 m.

2.2 Seismotectonics

Bangladesh occupies major part of the Bengal Basin Fig. 2, which is one of the largest sedimentary basins in the world [2, 31]. This pericratonic basin, as well as Bangladesh, in the northeast of the Indian shield, is surrounded in the north and east by actively converging plate boundaries of the Himalaya and the Burman Arcs, respectively [6, 7, 28, 31]. The tectonic condition of Bangladesh and its adjacent area have made this region potential for earthquake. Paleoseismic records and modern earthquake data in the foredeep areas of the Himalayan and Burman arcs suggest that active faults are bounding these blocks [7, 40]. These faults are also regarded as plate boundary faults Fig. 2. Record of several earthquakes around the Bengal Basin implies that this basin is seismically active.

Moulvibazar town lies in the greater Sylhet region where a number of earthquakes occurred in the past [4]. Geologically, this town is located in the Sylhet Basin which is also known as Surma Basin or Sylhet Trough [17]. Shillong Massif is in the north of the Sylhet Basin. The frontal deformation zone of the Burma Arc lies to the east of this basin [17]. The interplay between the rising Shillong Massif and the Indo-Burman fold belt is responsible for evolving this Miocene, actively subsiding basin [14]. Steckler et al. [40] and Morino et al. [25, 26] described the Dauki fault as a major active structure in this region.

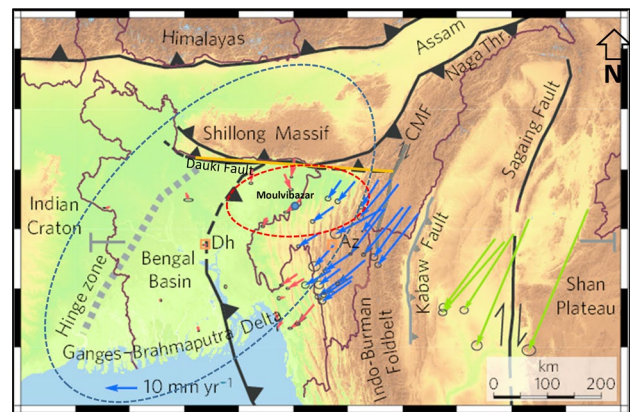


Fig. 2 Tectonic and paleoseismic map of Bangladesh. Bengal Basin is outlined by dotted blue circle, Surma Basin is demarcated by red circle, and Dauki Fault is represented by orange line Reproduced from Steckler et al. [41]

Table 1 Classification of the geological materials of Moulvibazar town according to the unified soil classification system (USCS)

Surface geological unit	USCS soil type	Geological age
Holocene flood plain deposits	CL, ML, SC, SM, SP	Holocene
Holo–Pleistocene low elevated terrace deposits	CH, CL, MH, ML, SM, SC, SP	Holo–Pleistocene

Bangladesh has been divided into four major seismic zones based on the peak horizontal ground acceleration (PGA) [8]. The zones are Zone I, Zone II, Zone III, and Zone IV, having PGA value of 0.12 g, 0.20 g, 0.28 g, and 0.36 g, respectively Fig. 3. Moulvibazar town lies within the Zone IV, which has PGA value of 0.36 g. It is notable that the Sylhet region has the maximum PGA value in the country, implying the most vulnerable zone for seismic hazard.

3 Methodology

The standard penetration test blow counts (SPT-N) are generally used worldwide to evaluate liquefaction potential analysis using design earthquake [9, 18, 31, 35, 47, 48]. The

simplified procedure [37], later updated, calibrated, and validated by Youd et al. [48], has been used for evaluating liquefaction potential from the SPT-N values of the geological materials of Moulvibazar town. Using the SPT-N values at each 1.5 m interval starting at a depth of 1.5 m from the ground surface to a depth of 20 m, the factor of safety against liquefaction (F_L) at each 1.5 m interval and liquefaction potential index (LPI) for each SPT-N profile down to a depth of 20 m have been calculated to observe the severity of liquefaction at each borehole site. The liquefaction hazard map of the study area has been prepared using the LPI values of the SPT-N profiles located at different surface geological units of the study area.

3.1 Dataset

The SPT-N profiles of 25 boreholes were used for this study. The SPT-N values and disturbed samples were collected from each borehole at each 1.5 m interval down to a depth of 20 m. Decision for the selection of boring sites has been made following the surface geological units of the area. The locations of the boreholes are manifested in the surface geological map of the study area Fig. 1. Among them, 5 boreholes are on the Holo–Pleistocene low elevated terrace deposits, and 20 boreholes are on the Holocene flood plain deposits.

The subsoils of each borehole down to a depth of 20 m are classified using Unified Soil Classification System (USCS). The groundwater level at each borehole was recorded after 24 h from the completion of the borehole, and topographic elevation was also recorded during the site investigation. The grain size distribution data are obtained by mechanical sieve analysis of coarse-grained soils and hydrometer analysis of fine-grained soils to determine the percentages of silt and clay. The groundwater level varies from 0.013 m to 3.5 m in the boreholes of the study area. In Table 2, the geological and geotechnical properties of a soil layer that are required for liquefaction potential analysis are shown from borehole Mlv-08 and the bore log of this borehole is presented in Fig. 4.

The epicenter of 1918 Srimangal Earthquake (M_w 7.6) was located about 30 km away from Moulvibazar town [42, 43]. According to the report of Stuart [42], all the brick buildings in Moulvibazar town were damaged and many of them were thrown down. The Moulvibazar town was in the area enclosed by Isoseist line no. 2 of the intensity map of the 8

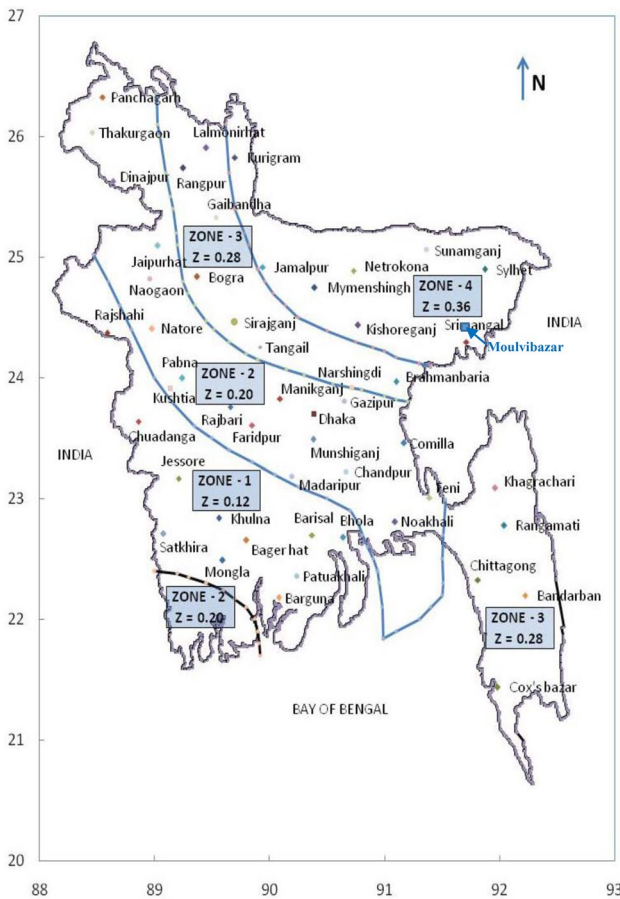
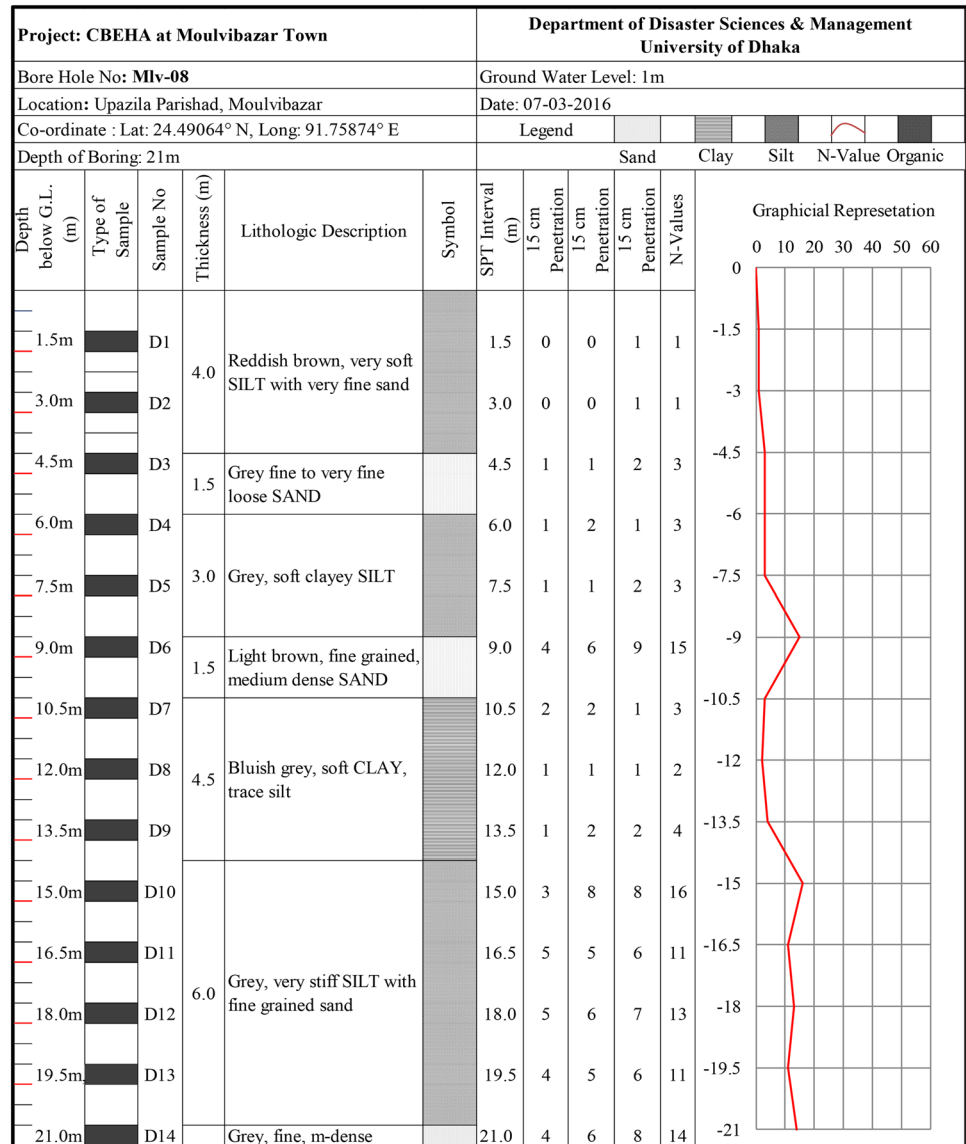


Fig. 3 Seismic zoning map of Bangladesh (BNBC 2014)

Table 2 Geological and geotechnical properties (geological age, lithology, soil type, fines content (FC), unit weight above groundwater level (γ_d), and unit weight below groundwater level (γ_t)) of a subsoil layer from borehole Mlv-08

Age	Lithology	Soil type	FC (%)	γ_d (kN/m ³)	γ_t (kN/m ³)	GWT (m)	Depth (m)	SPT N value
Recent	Silt	ML	90	14	17	1	1.5	1

Fig. 4 Borehole Mlv-08 (for example) showing lithological information with SPT-N values and groundwater level



July 1918 Srimangal Earthquake. The description of the damage in the area enclosed by Ioseist line no. 2 is comparable with VII to VIII in the MMI scale, which is equivalent to the PGA value of 0.15–0.25 g according to the relationship of Trifunac and Brady [44] and Tselentis and Danciu [45]. However, in the seismic zoning map of Bangladesh [8], the peak horizontal ground acceleration (PGA) for Moulvibazar town is assigned as 0.36 g. Therefore, we used the PGA value and earthquake magnitude as 0.36 g and M_w 8.0, respectively, for calculating the factor of safety (F_L) against liquefaction.

3.2 Calculation of factor of safety (F_L) against liquefaction

The factor of safety (F_L) against liquefaction is defined in terms of cyclic stress ratio (CSR), cyclic resistance ratio (CRR), and a magnitude scaling factor (MSF) [48]:

$$F_L = \left(\frac{CRR_{7.5}}{CSR} \right) MSF \tag{1}$$

$F_L > 1$ indicates a non-liquefiable soil layer, whereas $F_L < 1$ indicates a liquefiable one. The cyclic stress ratio, being proportional to the peak horizontal ground acceleration (a_{max}), is the amount of cyclic stress generated during an earthquake (cyclic loading). The cyclic resistance ratio, in contrary, is the required stress for changing the condition of a soil from solid to liquefied state for an earthquake of magnitude M_w 7.5 ($CRR_{7.5}$). The MSF is used to adjust the $CRR_{7.5}$ for other earthquake magnitudes. The standard penetration resistance $(N_1)_{60cs}$ of clean sand equivalent is used to calculate the $CRR_{7.5}$. An example of F_L calculation for borehole Mlv-08 is shown in Table 3.

The CSR [37] is expressed as:

$$CSR = 0.65 \times \left(\frac{a_{max}}{g}\right) \times \left(\frac{\sigma_t}{\sigma_{te}}\right) \times r_d \tag{2}$$

where a_{max} peak horizontal ground acceleration, g = gravitational acceleration, σ_t = total stress, σ_{te} = total effective stress, and r_d = stress reduction coefficient.

In this study, the term r_d was calculated by the following equation [48]:

$$r_d = \frac{(1.000 - 0.4113z^2 + 0.04052z + 0.001753z^{1.5})}{(1.000 - 0.4177z^{0.5} + 0.05729z - 0.006205z^{1.5} + 0.001210z^2)} \tag{3}$$

where z = depth below ground level.

The $CRR_{7.5}$ was calculated by the following equation [48]:

$$CRR_{7.5} = \frac{1}{34 - (N_1)_{60cs}} + \frac{(N_1)_{60cs}}{135} + \frac{50}{[10 \cdot (N_1)_{60cs} + 45]^2} - \frac{1}{200} \tag{4}$$

where the term $(N_1)_{60cs}$ is the normalized standard penetration test blow counts (SPT-N) to an overburden pressure of about 100 kPa, when a hammer energy ratio or

hammer efficiency is 60%, which is further corrected for fines content (FC) as follows [48]:

$$(N_1)_{60cs} = \alpha + \beta(N_1)_{60} \tag{5}$$

where α and β are the coefficients and determined by the following relationships:

$$\alpha = 0 \text{ For } FC \leq 5\% \tag{6a}$$

$$\alpha = \exp\left[1.76 - \frac{190}{FC^2}\right] \text{ For } 5\% < FC < 35\% \tag{6b}$$

$$\alpha = 5.0 \text{ For } FC \geq 35\% \tag{6c}$$

$$\beta = 1.0 \text{ For } FC \leq 35\% \tag{6d}$$

$$\beta = \exp\left[0.99 + \frac{FC^{1.5}}{1000}\right] \text{ For } 5\% < FC < 35\% \tag{6e}$$

$$\beta = 1.2 \text{ For } FC \geq 35\% \tag{6f}$$

The term $(N_1)_{60}$ denotes normalized SPT-N, adjusted to approximately 110 kPa overburden pressure that is further calculated by the equation below:

$$(N_1)_{60} = N_m C_N C_E C_B C_R C_s \tag{7}$$

where N_m = SPT-N value, C_N = N_m normalization factor regarding overburden stress, C_E = $60/100$ = corrected hammer energy ratio, C_B = borehole diameter correction factor, C_R = correction factor for rod length, and C_s = sampler correction.

Again, the term C_N is expressed mathematically as follows:

Table 3 Factor of safety (F_L) calculation for the subsoil profile of borehole Mlv-08

FC (%)	a_{max}	GWT(m)	σ_t (kPa)	σ_{te} (kPa)	r_d	CSR	Depth (m)	N_m	C_N	C_E	C_B	C_R	C_s	$(N_1)_{60}$	$(N_1)_{60cs}$	$CRR_{7.5}$	F_L
90	0.36	1.0	22.5	17.60	0.99	0.296	1.5	1	2.384	0.6	1	0.8	1	1.14	6.373	0.082	0.27
13	0.36		57.0	37.38	0.97	0.349	3.0	1	1.636	0.6	1	0.8	1	0.78	2.702	0.056	0.16
15	0.36		87.0	52.66	0.96	0.375	4.5	3	1.378	0.6	1	0.8	1	1.98	4.577	0.068	0.18
87	0.36		102.0	52.95	0.95	0.432	6.0	3	1.374	0.6	1	0.8	1	1.97	7.374	0.090	0.21
80	0.36		128.3	64.48	0.94	0.439	7.5	3	1.245	0.6	1	0.8	1	1.79	7.151	0.088	0.20
6	0.36		181.3	102.8	0.92	0.381	9.0	15	0.986	0.6	1	0.8	1	7.09	7.162	0.088	0.23
90	0.36		240.0	117.37	0.81	0.388	13.5	4	0.923	0.6	1	0.8	1	1.77	7.126	0.088	0.22
98	0.36		274.5	137.16	0.76	0.356	15.0	16	0.854	0.6	1	0.8	1	6.55	12.869	0.139	0.39
90	0.36		294.0	141.94	0.71	0.345	16.5	11	0.839	0.6	1	0.8	1	4.43	10.318	0.115	0.33
87	0.36		321.0	154.23	0.66	0.325	18.0	13	0.805	0.6	1	0.8	1	5.02	11.029	0.122	0.37
87	0.36		348.0	166.51	0.62	0.308	19.5	11	0.775	0.6	1	0.8	1	4.09	9.910	0.112	0.36
28	0.36		427.1	230.9	0.59	0.259	21.0	14	0.658	0.6	1	0.8	1	4.42	9.594	0.109	0.42

$$C_N = \left(\frac{P_a}{\sigma_{te}} \right)^{0.5} \quad (8)$$

where $P_a = 100$, because C_N normalizes N_m to an effective overburden pressure of about 100 kPa.

3.3 Calculation of liquefaction potential index (LPI)

The factor of safety (F_L) only determines whether a soil layer will liquefy or not. It is not possible to quantify the severity of liquefaction based on the factor of safety only. The severity of liquefaction can be quantified and categorized spatially using the liquefaction potential index (LPI). Therefore, the severity of liquefaction can be mapped using different LPI values that exist at different locations of an area [12].

Iwasaki et al. [15, 16] introduced thickness and depth of the susceptible soil layer in addition to F_L in the LPI calculation. The LPI is proportionally related to (1) the thickness of the liquefiable soil layer, (2) the distance between the susceptible soil layer and the ground surface, and (3) the difference of the factor of safety value from 1.0, when $F_L < 1$.

The LPI defined by Iwasaki et al. [16] is as follows:

$$LPI = \int_0^{20} F(z)W(z)dz \quad (9)$$

$$F(z) = 1 - F_L \text{ for } F_L < 1.0 \quad (10a)$$

$$F(z) = 0 \text{ for } F_L \geq 1.0 \quad (10b)$$

$$W(z) = 10 - 0.5z \text{ for } z < 20 \text{ m} \quad (10c)$$

$$W(z) = 0 \text{ for } z > 20 \text{ m} \quad (10d)$$

where z is the depth of the soil layer from the ground surface in meters.

According to Iwasaki et al. [16], the surface manifestation of liquefaction will occur where the $LPI \geq 5$, and liquefaction will be severe, where the $LPI > 15$. Holzer et al. [13] examined that the liquefaction triggered sand boils and lateral spreading were corresponding to the values of $LPI \geq 5$ and $LPI \geq 12$, respectively. Based on the LPI values, Iwasaki et al. [16] classified the severity of liquefaction as very low ($LPI = 0$), low ($0 < LPI \leq 5$), high ($5 < LPI \leq 15$), and very high ($LPI > 15$). Other such classifications schemes are also available [10, 18, 19, 21, 39]. However, for hazard mapping, we adopted the LPI-based liquefaction hazard categories of Iwasaki et al. [16], which has already been used by many authors [11, 32, 33].

Holzer et al. [12, 13] used the cumulative frequency distribution of the LPI values of a surface geological unit to

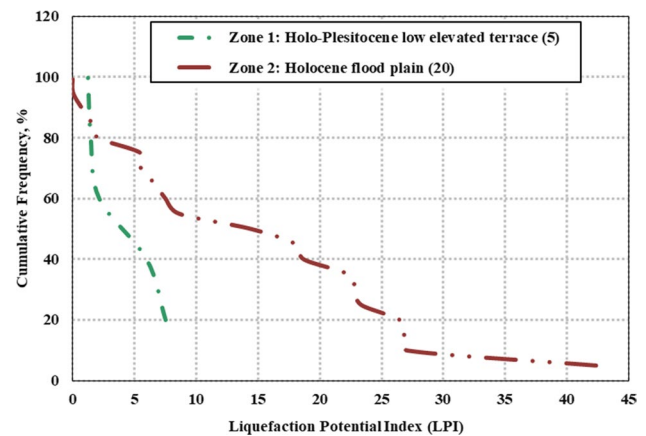


Fig. 5 Cumulative frequency distributions of LPI for two surface geological units of Moulvibazar town. Parentheses of the legend represent the number of SPT profiles used for each unit

predict the percentage of area of the unit that will show surface manifestation of liquefaction, when $LPI \geq 5$ Fig. 5.

4 Results and discussion

The LPI values of 25 SPT-N profiles and other information are provided in Table 4. The liquefaction hazard map for Moulvibazar town has been prepared based on the LPI values and cumulative frequency distribution of the LPI values for each unit Fig. 6. The contour lines of equal LPI values have been drawn at an interval of 5 LPI value to predict the LPI values for the areas where the SPT-N profiles are not available. The liquefaction hazard map also represents the likelihood of surface manifestation of liquefaction of each surface geological unit as percentage, where the LPI value is equal to or greater than 5. Thus, the study area is divided into two liquefaction hazard zones based on the surface geological units: Zone 1 (Holo–Pleistocene low elevated terrace deposits) and Zone 2 (Holocene flood plain deposits). Zone 1 covers southeastern corner of the mapped area that contains five LPI values, and Zone 2 covers rest of the mapped area that contains twenty LPI values.

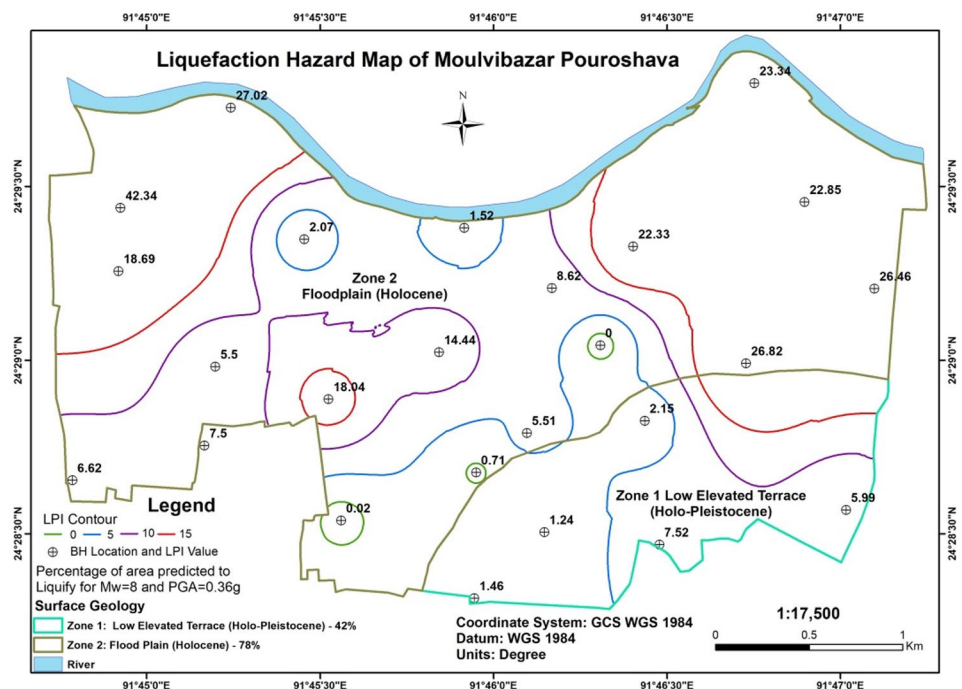
Cumulative frequency distribution of LPI is a quantitative approach to estimate how much area of a surface geological unit will show surface manifestation of liquefaction. Large and small percentage of area predicted to liquefy by cumulative frequency distribution of LPI is consistent with historical earthquake [12]. However, in Zone 1, 42% of the total area will show surface manifestation of liquefaction, whereas in Zone 2, 78% of total area will show surface manifestation of liquefaction.

The liquefaction hazard is classified based on the LPI-based hazard index of Iwasaki et al. [16]. The classification

Table 4 Calculated liquefaction potential index (LPI) of every SPT profile for a scenario seismic event of M_w 8 and PGA (a_{max}) of 0.36 g

Borehole no.	Coordinates		Elevation (m)	GWT (m)	Drilling depth (m)	LPI	Surface geology unit
	Latitude (N)	Longitude (E)					
Mlv-01	24.48041	91.77394	21	0.01	21.0	2.15	Holo–Pleistocene low elevated terrace
Mlv-02	24.47982	91.76828	17	0.50	21.0	5.51	Holocene flood plain
Mlv-03	24.48678	91.76947	18	1.00	21.0	8.62	Holocene flood plain
Mlv-04	24.47507	91.76911	13	0.20	21.0	1.24	Holo–Pleistocene low elevated terrace
Mlv-05	24.47794	91.76584	13	0.40	21.0	0.71	Holocene flood plain
Mlv-06	24.48301	91.7533	19	0.70	21.0	5.50	Holocene flood plain
Mlv-07	24.48913	91.75758	18	0.60	21.0	2.07	Holocene flood plain
Mlv-08	24.49064	91.74874	17	1.00	21.0	42.34	Holocene flood plain
Mlv-09	24.4837	91.76405	16	0.20	21.0	14.43	Holocene flood plain
Mlv-10	24.48404	91.77181	19	0.70	21.0	0.00	Holocene flood plain
Mlv-11	24.48878	91.77338	19	2.00	21.0	22.33	Holocene flood plain
Mlv-12	24.48317	91.77881	23	2.00	21.0	26.82	Holocene flood plain
Mlv-13	24.47447	91.77465	20	3.50	21.0	7.52	Holo–Pleistocene low elevated terrace
Mlv-14	24.48968	91.76527	20	1.50	21.0	1.52	Holocene flood plain
Mlv-15	24.47189	91.76575	13	2.00	21.0	1.46	Holo–Pleistocene low elevated terrace
Mlv-16	24.47563	91.75935	17	1.50	21.0	0.02	Holocene flood plain
Mlv-17	24.48145	91.75873	16	2.50	21.0	18.04	Holocene flood plain
Mlv-18	24.47923	91.75278	17	2.00	21.0	7.50	Holocene flood plain
Mlv-19	24.48759	91.74865	18	2.50	21.0	18.69	Holocene flood plain
Mlv-20	24.49544	91.75404	14	3.00	21.0	27.02	Holocene flood plain
Mlv-21	24.47756	91.74643	20	2.00	21.0	6.62	Holocene flood plain
Mlv-22	24.47613	91.78362	25	3.50	21.0	5.99	Holo–Pleistocene low elevated terrace
Mlv-23	24.48676	91.78498	15	2.00	21.0	26.46	Holocene flood plain
Mlv-24	24.49091	91.78162	19	1.00	21.0	22.85	Holocene flood plain
Mlv-25	24.49662	91.77921	17	3.00	21.0	23.34	Holocene flood plain

Fig.6 Liquefaction hazard map of Moulvibazar town. Liquefaction hazard potential is indexed as very low for $LPI=0$; low for $0 < LPI \leq 5$; high for $5 < LPI \leq 15$; and very high for $LPI > 15$. The 42% and 78% areas of Zone 1 and Zone 2, respectively, will show surface manifestation of liquefaction during a scenario earthquake of M_w 8 having peak horizontal ground acceleration (PGA) of 0.36 g



of liquefaction hazard for the mapped area is as follows: (1) very low for $LPI=0$, (2) low for $0 < LPI \leq 5$, (3) high for $5 < LPI \leq 15$, and (4) very high for $LPI > 15$.

From Fig. 6, it is observed that Zone 2 (Holocene flood plain deposits) shows higher LPI values than that of Zone 1 (Holo–Pleistocene low elevated terrace deposits). Therefore, the Holocene loose sandy and silty soils are more susceptible to liquefaction than that of the Pleistocene terrace deposits [21].

In Fig. 7, two borehole logs of two zones containing lithological and SPT-N value information are presented to show the variation in lithology and SPT-N values due to the sedimentary deposits of different geological age.

Holo–Pleistocene yellowish brown to reddish brown clay, clayey silt, and sand make up the upper 20 m of the subterranean soils of Zone 1. The presence of loose sandy soils with groundwater level at shallow depth increases the liquefaction susceptibility [1]. In Zone 1, the SPT values indicate that clayey soils are very soft to hard, and the sandy soils are loose to very dense in nature. Liquefaction potential analysis yields that this zone has very low to high liquefaction hazard, i.e., LPI

values from 1.24 to 7.52, Fig. 6. Usually, the Pleistocene sediments are less susceptible to liquefy. However, the Holocene deposits (1 m to 7 m thick) consisting of loose sandy to silty soils present in the valleys of the Pleistocene terrace reveal high liquefaction susceptibility. For example, during the 1886 Charleston earthquake, the Pleistocene sand deposits have been liquefied [22]. Holzer et al. [12] also revealed that the Pleistocene fan and sand deposits may liquefy during strong ground shaking. In the report of the 1918 Srimangal Earthquake, Stuart [42] mentioned that two small hollows were present on the ground of a tea factory that was located on the Pleistocene deposits close to the study area.

The Zone 2 (Holocene flood plain deposit) is comprised of, up to 20 m depth, light grey to dark grey clay, silty clay, silt, and sand. The clayey soils of this zone are very soft to hard, and sandy soils are very loose to very dense. The LPI values of this zone range from 0 to 42.34, indicating very low to very high liquefaction hazard. Low LPI values in the middle part of Zone 2 indicate that thick silty clay and clayey silt layers exist within 20 m depth at these borehole locations Fig. 6.

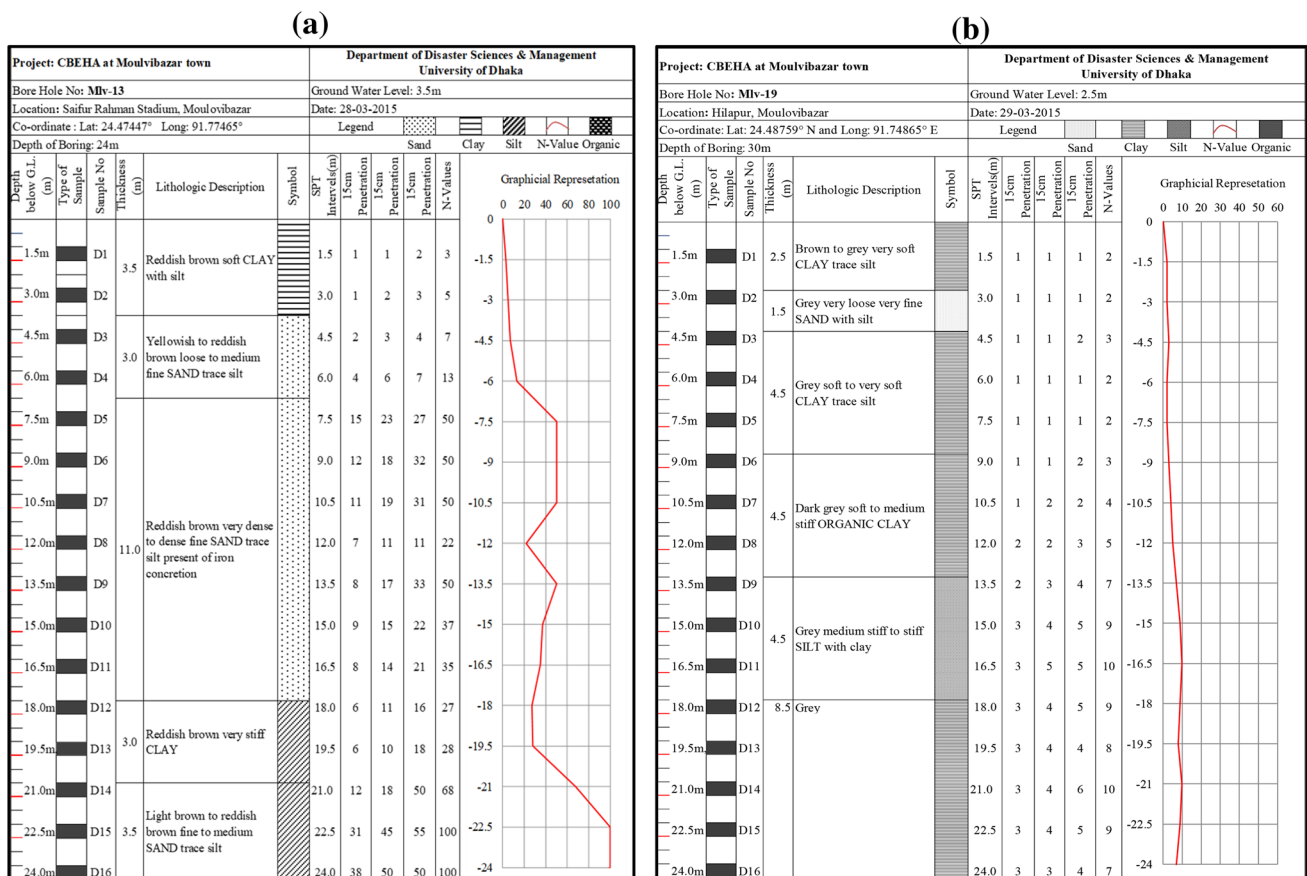


Fig. 7 Lithological logs with uncorrected SPT-N values: **a** Borehole No. Mlv-13 from Holo–Pleistocene terrace deposits (Zone 1) and **b** Borehole No. Mlv-19 from Holocene flood plain deposits (Zone 2)

Table 5 Liquefaction potential index (LPI) value changes with the depth of groundwater level (GWL)

BH no.	LPI at different groundwater level (GWL)							BH no.	LPI at different groundwater level (GWL)						
	0 m	1.5 m	3 m	4.5 m	6 m	9 m	10.5 m		0 m	1.5 m	3 m	4.5 m	6 m	9 m	10.5 m
1	2.15	1.88	1.67	1.54	1.51	0	0	14	2.00	1.52	1.22	0.92	0.61	0.05	0.00
2	5.56	5.42	5.29	5.15	5.01	4.73	4.59	15	1.86	1.56	1.26	0.94	0.62	0.00	0.00
3	8.88	8.49	8.10	7.69	7.27	0.15	0.15	16	0.02	0.02	0.01	0.01	0.01	0.01	0.02
4	1.24	1.20	1.16	1.11	1.06	0.97	0.92	17	20.29	18.99	9.73	9.31	1.95	1.84	1.78
5	0.77	0.54	0.32	0.12	0.00	0.00	0.00	18	7.77	7.57	7.36	7.13	6.90	0.00	0.00
6	5.79	5.17	4.54	3.90	3.26	1.94	1.26	19	20.08	19.28	8.26	8.01	7.74	7.19	6.89
7	2.13	1.97	1.79	1.61	1.43	1.03	0.82	20	30.73	28.94	27.02	19.00	14.12	9.49	4.30
8	49.08	34.61	22.68	13.81	8.35	1.40	1.04	21	6.82	6.67	6.51	6.35	6.17	0.00	0.00
9	14.92	11.18	7.15	2.28	2.03	1.50	1.21	22	9.38	7.94	6.40	0.23	0.00	0.00	0.00
10	0.00	0.00	0.00	0.00	0.00	0.00	0.00	23	28.49	27.00	15.85	6.91	6.53	5.71	5.28
11	23.95	22.75	21.45	12.03	5.11	4.67	4.46	24	24.30	22.95	22.07	12.03	5.11	4.67	4.46
12	28.82	27.35	16.22	7.29	6.92	6.14	5.73	25	26.69	25.07	23.34	15.51	10.82	6.62	6.43
13	10.48	9.27	7.97	1.81	1.55	1.01	0.72								

The groundwater level plays an important role in calculating factor of safety (F_L) and LPI values [10]. The SPT borings of this study were performed during monsoon, when groundwater level of this area was at shallow depth (0.013 m to 3.5 m). The groundwater level at shallow depth has eventually increased the LPI values and surface manifestation of liquefaction Table 5.

The epicenter of the 1918 Srimangal Earthquake (M_w 7.6) was located within a radius of 30 km from Moulvibazar town. During Srimangal Earthquake, widespread spouting out of sand and water (liquefaction) was reported within a radius of more than 100 km (Sylhet, Agartala, Comilla, Kishoreganj, and Netrokona) from the epicenter [42]. Our study also suggests that widespread and severe liquefaction would occur in the saturated sandy and silty soils of the Quaternary (Pleistocene and Holocene) alluvium of Moulvibazar town during a scenario earthquake of M_w 8 having a peak horizontal ground acceleration (PGA) of 0.36 g in Moulvibazar town. Lee et al. [20], Holzer et al. [12], and Rahman et al. [31] also predicted that severe liquefaction would occur in the Quaternary (Pleistocene and Holocene) sandy and silty alluvium during a scenario earthquake of magnitude greater than M_w 7 having a peak horizontal ground acceleration (PGA) of greater than 0.15 g.

5 Conclusions

In this study, we have assessed liquefaction susceptibility of subsurface geological materials of Moulvibazar town using liquefaction potential index (LPI) from geotechnical properties of soil and groundwater depth, and subsequently prepared a hazard map for a scenario earthquake

of magnitude 8.0 M_w having a peak horizontal ground acceleration (PGA) of 0.36 g. The SPT N values and soil samples from 25 boreholes were used for this study. Factor of safety of each soil layer of the SPT profiles was calculated using the simplified procedure, and the factor of safety of all layers encountered in a borehole down to a depth of 20 m was summed up to calculate the LPI value for a borehole. From field survey and borehole investigations, two surface geological units were identified in the study area: (1) Holo–Pleistocene low elevated terrace deposits and (2) Holocene flood plain deposits, and they were denoted as two hazard zones, i.e., Zone 1 and Zone 2, respectively. The liquefaction hazard map represents spatial variation of degree of hazard by means of contour lines of equal values. The LPI values vary from 0 to 42.33 within the town, whereas values from 1.42 to 7.52 are in Zone 1 and values from 0 to 42.34 are in Zone 2. Thus, Zone 1 represents very low to high and Zone 2 shows very low to very high liquefaction hazard potential. The cumulative percentages of LPI revealed that 42% and 78% of the surface areas of Zone 1 and Zone 2, respectively, would exhibit surface manifestation of liquefaction during a scenario earthquake of magnitude 8.0 M_w having a PGA of 0.36 g.

The liquefaction hazard map of Moulvibazar town can be used for site-specific seismic site characterization and microzonation, and guidelines preparation for planners and policy makers for seismic risk management of Moulvibazar town.

Acknowledgements The authors convey their gratitude to the Ministry of Science and Technology, Bangladesh, for funding the research project “Capacity building for earthquake induced liquefaction hazard assessment at Moulvibazar Pourashava, Sylhet, Bangladesh.” They are also thankful to the Department of Disaster Science and Management, University of Dhaka, for further support. The authors would like

to acknowledge the Department of Geology, University of Dhaka, for permitting to use the facilities of Engineering Geology Laboratory.

Compliance with ethical standards

Conflict of interest On behalf of all authors, the corresponding author states that there is no conflict of interest.

References

- Ahmad M, Tang XW, Ahmad F, Jamal A (2018) Assessment of soil liquefaction potential in Kamra, Pakistan. *Sustainability* 10:1–16. <https://doi.org/10.3390/su10114223>
- Alam M, Alam MM, Curray JR (2003) An overview of the sedimentary geology of the Bengal Basin in relation to the regional tectonic framework and basin-fill history. *Sediment Geol* 155:179–208
- Alam MK, Hasan AKMS, Khan MR, Whitney JW (1990) Geological map of Bangladesh. Geological Survey of Bangladesh, Dhaka
- Ansary MA, Islam MR (2008) Seismic microzonation of Sylhet city. *J South Asia Disaster Stud* 1:179–195
- BBS (2013) District Statistics 2011 (Moulvibazar), Bangladesh Bureau of Statistics (BSS), Statistics and Information Division (SID), Ministry of Planning, Government of the People's Republic of Bangladesh
- Bilham R (2004) Earthquakes in India and the Himalaya: tectonics, geodesy and history. *Ann Geophys* 47:839–858. <https://doi.org/10.4401/ag-3338>
- Bilham R, England P (2001) Plateau “pop-up” in the great 1897 Assam earthquake. *Nature* 410:806–809. <https://doi.org/10.1038/35071057>
- BNBC (2014) Bangladesh National Building Code. Housing and Building Research Institute (draft report)
- Cetin KO, Seed RB, Der Kiureghian A et al (2004) Standard penetration test-based probabilistic and deterministic assessment of seismic soil liquefaction potential. *J Geotech Geoenviron Eng* 130:1314–1340. [https://doi.org/10.1061/\(ASCE\)1090-0241\(2004\)130:12\(1314\)](https://doi.org/10.1061/(ASCE)1090-0241(2004)130:12(1314))
- Chao SJ, Hsu HM, Hwang H (2010) Soil liquefaction potential in Ilan City and Lotung Town. *Taiwan J Geoenviron* 5:21–27. [https://doi.org/10.6310/jog.2010.5\(1\).3](https://doi.org/10.6310/jog.2010.5(1).3)
- Farazi AH, Ferdous N, Kamal ASMM (2018) LPI-based earthquake-induced soil liquefaction susceptibility assessment at Probashi Palli Abasan Project Area, Tongi, Gazipur, Bangladesh. *J Sci Res* 10:105–116. <https://doi.org/10.3329/jsr.v10i2.34225>
- Holzer TL, Bennett MJ, Noce TE et al (2006) Liquefaction hazard mapping with LPI in the Greater Oakland, California, area. *Earthq Spectra* 22:693–708. <https://doi.org/10.1193/1.2218591>
- Holzer TL, Toprak S, Bennett M (2003) Application of the liquefaction potential index to liquefaction hazard mapping. Eighth US–Japan Workshop on Earthquake Resistant Design of Lifeline Facilities and Countermeasures against Liquefaction, pp 161–171
- Hossain HMZ, Roser BP, Kimura J-I (2010) Petrography and whole-rock geochemistry of the Tertiary Sylhet succession, northeastern Bengal Basin, Bangladesh: provenance and source area weathering. *Sediment Geol* 228:171–183. <https://doi.org/10.1016/j.sedgeo.2010.04.009>
- Iwasaki T, Tatsuoka F, Tokida K -i, Yasuda S (1978) A practical method for assessing soil liquefaction potential based on case studies at various sites in Japan. In: Proceedings of 2nd international conference on microzonation. San Francisco, pp 885–896
- Iwasaki T, Tokida K, Tatsuoka F, et al (1982) Microzonation for soil liquefaction potential using simplified methods. In: Proceedings of 3rd international earthquake microzonation conference, pp 1319–1330
- Johnson SY, Alam AMN (1991) Sedimentation and tectonics of the Sylhet trough, Bangladesh. *Geol Soc Am Bull* 103:1513–1527. [https://doi.org/10.1130/0016-7606\(1991\)103%3c1513:SATOTS%3e2.3.CO;2](https://doi.org/10.1130/0016-7606(1991)103%3c1513:SATOTS%3e2.3.CO;2)
- Juang CH, Chen CJ, Jiang T, Andrus RD (2000) Risk-based liquefaction potential evaluation using standard penetration tests. *Can Geotech J* 37:1195–1208. <https://doi.org/10.1139/t00-064>
- Ku CH, Lee DH, Wu JH (2004) Evaluation of soil liquefaction in the Chi–Chi, Taiwan earthquake using CPT. *Soil Dyn Earthq Eng* 24:659–673
- Lee DH, Ku CS, Yuan H (2004) A study of the liquefaction risk potential at Yuanlin. *Taiwan Eng Geol* 71:97–117. [https://doi.org/10.1016/S0013-7952\(03\)00128-5](https://doi.org/10.1016/S0013-7952(03)00128-5)
- Lee YF, Chi YY, Lee DH et al (2007) Simplified models for assessing annual liquefaction probability—a case study of the Yuanlin area. *Taiwan Eng Geol* 90:71–88. <https://doi.org/10.1016/j.enggeo.2006.12.003>
- Martin JRI, Clough GW (1990) Implication from a geotechnical investigation of liquefaction phenomena associated with seismic events in the Charleston, SC area. Reston, VA
- Middlemiss CS (1885) Report on the Bengal earthquake of July 14, 1885. *Rec Geol Surv India* 18(4):200–221
- Mondal DR, McHugh CM, Mortlock RA et al (2018) Microatolls document the 1762 and prior earthquakes along the southeast coast of Bangladesh. *Tectonophysics* 745:196–213. <https://doi.org/10.1016/j.tecto.2018.07.020>
- Morino M, Kamal ASMM, Akhter SH et al (2014) A paleo-seismological study of the Dauki fault at Jaflong, Sylhet, Bangladesh: historical seismic events and an attempted rupture segmentation model. *J Asian Earth Sci* 91:218–226. <https://doi.org/10.1016/j.jseaes.2014.06.002>
- Morino M, Kamal ASMM, Muslim D et al (2011) Seismic event of the Dauki fault in 16th century confirmed by trench investigation at Gabrakhari village, Haluaghat, Mymensingh, Bangladesh. *J Asian Earth Sci* 42:492–498. <https://doi.org/10.1016/j.jseaes.2011.05.002>
- Morino M, Monsur MH, Kamal ASMM et al (2014) Examples of paleo-liquefaction in Bangladesh. *J Geol Soc Japan* 120:VII–VIII. <https://doi.org/10.5575/geosoc.2014.0032>
- Ni JF, Guzman-Speziale M, Bevis M et al (1989) Accretionary tectonics of Burma and the three-dimensional geometry of the Burma subduction zone. *Geology* 17:68–71
- Oldham RD (1899) Report on the great earthquake of 12th June 1897. *Memoirs of the Geological Survey of India*, p 29
- Papathanassiou G, Voudouris K, Christaras B, Pavlides S (2006) Prediction methods of earthquake-induced liquefaction surface manifestations. International association for mathematical geology. XIth international congress, pp 3–8
- Rahman M, Siddiqua S, Kamal A (2015) Liquefaction hazard mapping by liquefaction potential index for Dhaka City, Bangladesh. *Eng Geol* 188:137–147. <https://doi.org/10.1016/j.enggeo.2015.01.012>
- Rahman MZ, Hossain MS, Kamal ASMM et al (2018) Seismic site characterization for Moulvibazar town, Bangladesh. *Bull Eng Geol Environ* 77:1451–1471. <https://doi.org/10.1007/s10064-017-1031-6>
- Rahman Z, Siddiqua S (2016) Liquefaction resistance evaluation of soils using standard penetration test blow count and shear wave velocity. In: Proceedings of the 69th Canadian geotechnical society. Canadian Geotechnical Society, Vancouver, Canada, paper no. 3715

34. Sassa S, Takagawa T (2019) Liquefied gravity flow-induced tsunami: first evidence and comparison from the 2018 Indonesia Sulawesi earthquake and tsunami disasters. *Landslides* 16:195–200. <https://doi.org/10.1007/s10346-018-1114-x>
35. Seed HB, de Alba P (1986) Use of SPT and CPT tests for evaluating the liquefaction resistance of sands. In: Clemence SP (ed) *Use of in situ tests in geotechnical engineering*. American Society of Civil Engineers, Geotechnical Special Publication, vol 6, pp 281–302
36. Seed HB, Idriss IM (1967) Analysis of soil liquefaction: Niigata earthquake. *J Soil Mech Found Div* 93:83–108
37. Seed HB, Idriss IM (1971) Simplified procedure for evaluating soil liquefaction potential. *J Soil Mech Found Div* 97:1249–1273
38. Seed RB, Riemer MF, Dickenson SE (1991) Liquefaction of soils in the 1989 Loma Prieta earthquake. In: 2nd international conference on recent advances in geotechnical earthquake engineering and soil dynamics. Louis, Missouri, paper no. LP02
39. Sonmez H, Gokceoglu C (2005) A liquefaction severity index suggested for engineering practice. *Environ Geol* 48:81–91. <https://doi.org/10.1007/s00254-005-1263-9>
40. Steckler MS, Akhter SH, Seeber L (2008) Collision of the Ganges–Brahmaputra Delta with the Burma Arc: implications for earthquake hazard. *Earth Planet Sci Lett* 273:367–378. <https://doi.org/10.1016/j.epsl.2008.07.009>
41. Steckler MS, Mondal DR, Akhter SH et al (2016) Locked and loading megathrust linked to active subduction beneath the Indo-Burman Ranges. *Nat Geosci* 9:615–618. <https://doi.org/10.1038/ngeo2760>
42. Stuart M (1920) The Srimangal earthquake of 8th July 1918. *Memoirs of the Geological Survey of India* 46(1)
43. Szeliga W, Hough S, Martin S, Bilham R (2010) Intensity, magnitude, location, and attenuation in India for felt earthquakes since 1762. *Bull Seismol Soc Am* 100:570–584. <https://doi.org/10.1785/0120080329>
44. Trifunac MD, Brady AG (1975) On the correlation of seismic intensity scales with the peaks of recorded strong ground motion. *Bull Seismol Soc Am* 65:139–162
45. Tselentis GA, Danciu L (2008) Empirical relationships between modified Mercalli intensity and engineering ground-motion parameters in Greece. *Bull Seismol Soc Am* 98:1863–1875. <https://doi.org/10.1785/0120070172>
46. Walsh TJ, Combellick RA, Black GL (1995) Liquefaction features from a subduction zone earthquake: preserved examples from the 1964 Alaska earthquake
47. Yalcin A, Gokceoglu C, Sönmez H (2008) Liquefaction severity map for Aksaray city center (Central Anatolia, Turkey). *Nat Hazards Earth Syst Sci* 8:641–649. <https://doi.org/10.5194/nhess-8-641-2008>
48. Youd TL, Idriss IM, Andrus RD et al (2001) Liquefaction resistance of soils: summary report from the 1996 NCEER 14 and 1998 NCEER/NSF workshop on evaluation of liquefaction resistance of soils. *J Geotech Geoenviron Eng* 127:817–833

Publisher's Note Springer Nature remains neutral with regard to jurisdictional claims in published maps and institutional affiliations.